*Sensors and Materials*, Vol. 38, No. 7 (2026) 3979–3990
MYU Tokyo



S & M 4545

# Alternating Current Etching Method for Fabrication of High-performance Aluminum Electrolytic Capacitors

Yu-Chi Lin,[1] Teen-Hang Meen,[2*] Tung-Lung Wu,[3]
Min-Lang Yang,[4] and Kao-Wei Min[5**]

[1]College of Engineering, National Formosa University, Huwei, Yunlin 632, Taiwan
[2]Department of Electronic Engineering, National Formosa University, Huwei, Yunlin 632, Taiwan
[3]Department of Electrical Engineering, Lunghwa University of Science and Technology, Guishan District, Taoyuan City 333, Taiwan
[4]Department of Civil Engineering and Geomatics, Cheng Shiu University, Kaohsiung 833, Taiwan
[5]Department of Electrical Engineering, Cheng Shiu University, Kaohsiung 833, Taiwan

(Received August 21, 2025; accepted July 15, 2026)

***Keywords:*** AC etching, aluminum foil, sensor, capacitor

We optimized a multistage electrochemical etching method for fabricating high-performance aluminum electrolytic capacitors using alternating current (AC) to maximize electrostatic capacitance while preserving the mechanical properties of high-purity aluminum foil. The etching process was systematically investigated under various AC frequencies, current densities, durations, solution compositions, and aluminum ion concentrations. Pretreatment and chemical modification with phosphoric acid ($H_3PO_4$) provided a highly uniform corrosion pit distribution, preventing localized over-dissolution. The optimal etching conditions were identified as a solution containing 350 mL/L HCl, 15 mL/L $HNO_3$, 15 mL/L $H_3PO_4$, and 5 g/L $Al^{3+}$, a temperature of 35 °C, a current density of 0.6 A/cm$^2$, and a four-stage frequency-stepping profile of 30–30–25–20 Hz for a total etching time of 120 s. Under these conditions, the 50-μm-thick aluminum foil (99.99% purity) achieved a peak specific capacitance of 510.2 μF/cm$^2$, indicating a >20% improvement over conventional single-stage methods. Microstructural analysis revealed a highly dense pit network with an average pit diameter of 180–240 nm, a nucleation density of $4.2 \times 10^9$ pits/cm$^2$, an average surface roughness of 1.68 μm, and an exceptional surface enlargement factor of approximately 96.5. Lattice orientations of [220], [311], [200], and [422] in this order contributed to this surface expansion. Process reliability was confirmed by a low capacitance coefficient of variation (<1.2%), whereas the etched foil retained over 75% of its pristine tensile strength. Electrical evaluations demonstrated an exceptionally low equivalent series resistance of 0.12 Ω at 120 Hz, a superior frequency response (68% capacitance retention at 1 kHz), and a robust stability under accelerated life testing (85 °C at a rated voltage of 6.3 V for 1000 h) with less than 4.5% degradation. These results show that this multistage AC etching method directly supports the miniaturization, signal stability, and ruggedization demands of next-generation intelligent sensor technologies, particularly for localized power filtering in automotive modules and low-power wireless networks.

*Corresponding author: e-mail: thmeen@gs.nfu.edu.tw
**Corresponding author: e-mail: 8373@gcloud.csu.edu.tw
https://doi.org/10.18494/SAM5903

ISSN 0914-4935 

## 1. Introduction

A capacitor is a simple component that comprises an electrical insulator between two opposing electrodes. When a direct current (DC) voltage is applied across the two electrodes, the current flows into the capacitor until it reaches the supply voltage. Owing to the insulator, positive charges accumulate on the anode, whereas negative charges accumulate on the cathode to store electric charge.

When using materials such as Al (Al) or tantalum (Ta) for the electrodes, voltage-resistant oxide films are formed through electrolytic reactions, which is the principle underlying the fabrication of the Al or Ta electrolytic capacitor. In particular, Al electrolytic capacitors are widely used in electronic instruments as a major passive component to store electric charges in sensors. Al electrolytic capacitors ensure accurate readings and reliable operation, and enable bulk energy storage, control ripple and spikes from switch-mode supplies, and provide steady excitation rails, which are essential for sensors. They also provide high capacitance in compact volumes, which is ideal for power smoothing and decoupling around sensors and microcontroller units. Therefore, Al electrolytic capacitors are widely used in automotive sensor modules and low-power wireless sensors.[1–3]

Etched foils are widely adopted owing to their high capacitance density and dense tunnel structures on [100]-oriented Al, which have up to $10^7$ tunnels in a square centimeter, 1–2 μm width, and 40–50 μm length. A larger surface area means more charges in less space, which leads to the miniaturization of sensor modules or larger filtering headroom. A balance between forming and operating voltages (overanodization) and thinner and optimized separators and cathode foils with tailored electrolytes enables Al electrolytic capacitors to have operating reliability, extended working life, and enhanced ripple-current ratings.[3,4] Their higher specific capacitance and lower equivalent series resistance also enable smaller bulk caps and free space for sensors to be appropriate for local decoupling that lowers supply impedance at the load point. Therefore, it is important to form dense corrosion pits on the Al foil used in Al electrolytic capacitors.

Whereas conventional DC etching remains a standard approach to developing deep tunnel-type corrosion pits along the [100] orientation, it requires thicker foils but fails to achieve a uniform distribution of microscale voids over large surface areas without sacrificing mechanical strength.[5] On the other hand, classic single-frequency alternating current (AC) etching produces highly complex, dense pit structures but has limitations regarding structural breakdown and over-etching at prolonged exposure or elevated current densities.[6] These limitations can be overcome by implementing a novel four-stage frequency-stepping AC etching method (30–30–25–20 Hz) combined with a tailored multi-acid solution of hydrochloric acid (HCl), nitric acid ($HNO_3$), and phosphoric acid ($H_3PO_4$). This multistage step-down method is used to effectively manage pit nucleation in the initial high-frequency stages and pit growth in the lower-frequency stages to maximize electrostatic capacitance while ensuring a uniform corrosion distribution across high-purity aluminum foils.

In this study, we employed an AC etching method to increase the surface area and electrostatic capacitance of the Al electrolytic capacitor. The method minimizes material costs through an economical electrode processing technology, while it ensures the advantages of the capacitor, which are well-suited for industrial and automotive sensor modules.

## 2. Data, Materials, and Methods

The ratio of electric charge ($Q$) to the applied voltage ($V$) is used to define the capacitance ($C$) as follows.[5]

$$C = \frac{Q}{V} = \varepsilon \times \frac{A}{d}, \tag{1}$$

where the capacitance of a capacitor is equal to the dielectric constant ($\varepsilon$) multiplied by the surface area of the opposing electrodes ($A$), divided by the distance between the electrodes ($d$). To obtain a high-capacitance Al electrolytic capacitor, the surface area of the electrode material must be increased by subjecting the smooth surface of the electrode to create a rough and irregular surface to hold more electric charge and increase capacitance. This can be achieved by using an electrochemical or chemical etching process to construct the capacitor structure presented in Fig. 1. A flat aluminum foil is placed in a chemical solution with hydrochloric acid as the main agent, and phosphoric acid and nitric acid used as auxiliary agents. Direct current or alternating current is applied to the surface of the aluminum foil to perform electrochemical etching, so as to create porous corrosion holes and increase the specific surface area of the aluminum foil.

Al anode foils are categorized into high (375–600 V), medium (120–375 V), and low voltage (below 120 V) types. High-purity (99.99%) Al foil with a thickness of 80–115 μm is used for AC or DC electrochemical etching. On the other hand, the Al cathode foil is made of low-purity Al (99.4–99.9%) with a thickness of 20–50 μm and is fabricated through electrochemical or chemical etching. Al is an amphoteric material that is corroded by acids and bases. Alkaline solutions such as sodium hydroxide are commonly used for surface cleaning owing to their effectiveness in removing oxides and contaminants, but they are rarely employed in corrosion treatments. The alkaline solution dissolves Al uniformly, resulting in minimal surface texturing or localized attack. In contrast, acidic solutions, especially HCl, penetrate the oxide layer on the Al surface, causing localized corrosion and forming corrosion pits. Under the acidic condition, the chloride ions ($Cl^-$) in HCl react with Al ions ($Al^{3+}$) to form aluminum chloride ($AlCl_3$), which dissolves in the chemical corrosion solution. Meanwhile, hydrogen ions ($H^+$) are released as

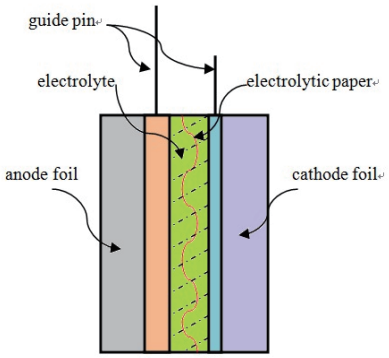


Fig. 1. (Color online) Simple structure diagram of Al electrolytic capacitor.[5,6]

hydrogen gas ($H_2$) into the air. This process only applies to low-purity Al foil. It is ineffective on high-purity Al foil owing to the foil's denser oxide film and lower content of alloying elements, which makes it difficult to form cells that are essential for corrosion initiation. Therefore, chemical etching does not yield the desired effect on high-purity Al foil.

In the electrochemical etching method, AC and DC or their hybrid is used in the etching process. In the DC etching method, the Al foil is placed in the etching solution and connected to the anode, while a carbon plate is connected to the cathode. In the method, the power supply, temperature of the etching solution, and the current density determine the dissolution rate of the Al foil. Using the DC etching method, tunnel-type corrosion pits are produced along the [100] lattice orientation.[6,7] In the AC etching method, AC induces cyclic anodic and cathodic reactions, which dissolve $Al^{3+}$ into the chemical solution and result in the formation of numerous pits on the Al foil surface.[8] In this method, current frequency and density significantly affect the formation of surface corrosion pits.[9] The method is characterized by the effective control of pit uniformity through adjustments of frequency, waveform, current density, and chemical composition, thereby enlarging the surface area. The size and shape of the pits formed depend significantly on electrochemical parameters, including current frequency and density.[10,11] The electrochemical method produces more complex and uniform pit structures than the chemical etching methods.

In this study, we formed dense corrosion pits on Al foil in an Al electrolytic capacitor using different AC etching methods under different conditions to increase the surface area and electrostatic capacitance. After pretreating the Al foil with 0.25 mole/L HCl, $H_3PO_4$, and $HNO_3$, and rinsing it with tap water to remove residual chemicals, the foil was immersed in an etching solution (a 2.5–8 mole/L mixture of 100–500 mL/L hydrochloric acid (HCl), 4–40 mL/L nitric acid ($HNO_3$), 10–50 mL/L $H_3PO_4$, and 1–8 g/L $Al^{3+}$) at a temperature of 20 to 45 °C. AC etching was then applied to form pits on the foil surface and increase the effective surface area. The Al foil was etched in four stages. In stages A–D, different AC frequencies (20–60 Hz) were applied for 30 s at a current density of 0.6 A/cm² and under AC power at 30-s intervals (Fig. 2).

Following AC etching, the foil was rinsed with tap water, then treated in a post-treatment solution (0.6 mole/L $HNO_3$) to remove residual chloride ions in the pits. Finally, the foil was rinsed with deionized water and dried at ambient temperature to remove moisture. The process for AC etching is summarized in Table 1. The capacitance of the foil was measured at 30 °C using an inductance, capacitance, and resistance meter in a solution of 150 g of ammonium adipate dissolved in 1000 mL of deionized water, following Japan's EIAJ-RC2364 standard for

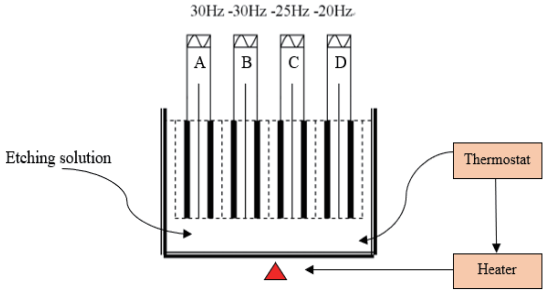


Fig. 2. (Color online) Schematic of AC etching method in four stages (A–D) of AC application used in this study.

Table 1
AC etching process and parameters.

| Step | Process | Current density (A/cm$^2$) | Etching time (s) | Temperature (°C) | Etching solution |
|---|---|---|---|---|---|
| 1 | Pretreatment | – | 60 | 60 | 0.25 mole/L ($H_3PO_4$) |
| 2 | Rinse | – | 30 | | Water |
| 3 | Etching | 0.3–1 | 100–180 | 35–45 | 2.5–8.0 mole/L ($HCl/HNO_3/H_3PO_4$) |
| 4 | Rinse | – | 30 | | Water |
| 5 | Post-treatment | – | 60 | 60 | 0.6 mole/L ($HNO_3$) |
| 6 | Rinse | – | 30 | | Deionized water |
| 7 | Dry | – | 60 | 120 | – |

capacitor electrostatic capacity. Etched foils of 1 × 1 cm$^2$ (width × length) size were gold-coated using an ion sputter coater to obtain the highest capacitance. Their pit morphology was observed by scanning electron microscopy (SEM). The capacitance of the AC-etched Al electrolytic capacitor was measured under different experimental conditions to examine the effects of etching solution composition, etching temperature and time, AC frequency, current density, and Al foil thickness.

## 3. Result

We measured the capacitance of the AC-etched Al electrolytic capacitor with the Al foil etched at different AC frequencies, current densities, etching times, etching solution mixtures, and $Al^{3+}$ amounts at a temperature between 30 and 45 °C. Before etching, the natural oxide layer on the Al foil surface was removed by immersing the foil in a 0.25 mol/L solution of HCL, $H_3PO_4$, or $HNO_3$ for 60 s. Figures 3(a) and 3(b) show the surface of Al foils pretreated with different acids, presenting a non-uniform distribution of corrosion pits. The surface of Al foils treated with $H_3PO_4$ showed the most uniform pit distribution [Fig. 3(c)].

Etching at 60 Hz produced larger corrosion pits than at 30 Hz of AC frequency. However, the etched surface at 60 Hz lacked uniformity in pit distribution, whereas 30 Hz yielded more consistent results [Figs. 4(a) and 4(b)].

When using a mixture of HCl and $HNO_3$ [Fig. 5(a)], the corrosion pits were irregularly distributed. The addition of $H_3PO_4$ significantly enhanced the uniformity of the corrosion pits on the Al foil surface [Fig. 5(b)].

We measured the capacitance of the AC-etched Al electrolytic capacitor using the mixed solution of 250 mL/L HCl, 3 mL/L $HNO_3$, 5 mL/L $H_3PO_4$, and 5g /L $Al^{3+}$ at the solution temperature of 35–45 ℃. The thickness of the Al foil was 95 μm, and its purity was 99.99%, with trace amounts of iron (0.006%) and copper (0.002%). The lattice orientations of the etched Al surface included [220] (74%), [311] (18%), [422] (7%), and [200] (6%). The four-stage frequencies of AC, the etching times, and current density were fixed at 60 Hz, 120 s, and 0.6 A/cm$^2$, respectively. Under these conditions, the capacitance did not increase with the temperature of the etching solution. The optimal temperature for AC etching was 35 ℃, whereas the optimal AC frequencies in stages A–D were 30, 30, 25, and 20 Hz, respectively, leading to the capacitances of 435 and 535 μF/cm$^2$ (Tables 2 and 3, respectively, and Fig. 6).

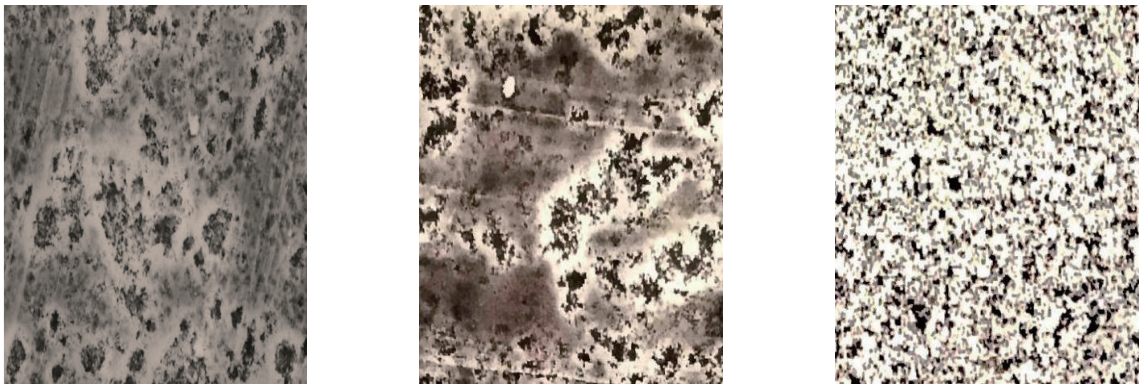

(a) (b) (c)

Fig. 3. (Color online) Pit morphology of AC-etched Al foil surface after pretreatment in (a) HCl, (b) $HNO_3$, and (c) $H_3PO_4$.

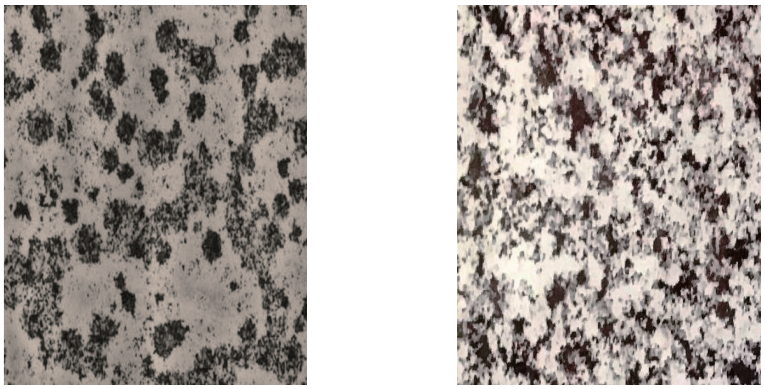

(a) (b)

Fig. 4. (Color online) Pit morphology of AC-etched Al foil surface after pretreatment in (a) HCl+$HNO_3$ and (b) HCl+$HNO_3$+$H_3PO_4$.

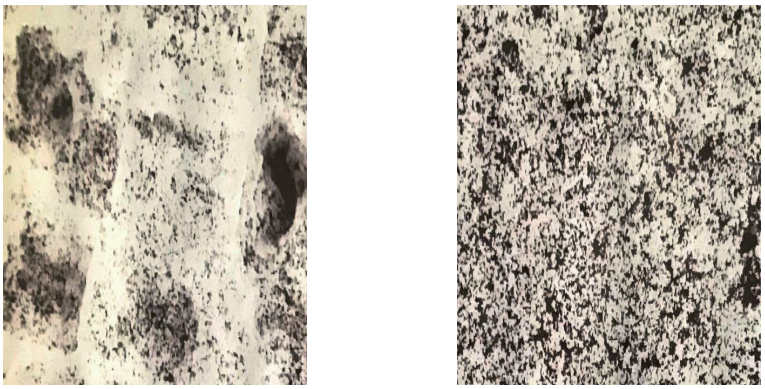

(a) (b)

Fig. 5. (Color online) Pit morphology of AC-etched Al foil surface at AC frequencies of (a) 60 and (b) 30 Hz.

Table 2
Capacitance of AC-etched Al electrolytic capacitor at different temperatures and etching times.

| Samples | Temperature (°C) | Etching time (s) | Capacitance (μF/cm$^2$) |
|---|---|---|---|
| 1 | 35 | 120 | 435 |
| 2 | 40 | 120 | 430 |
| 3 | 45 | 120 | 390 |

Table 3
Capacitance results of AC-etched Al electrolytic capacitor at different temperatures, etching times, and AC frequencies.

| Sample | Temperature (°C) | Frequency (Hz) | Etching time (s) | Capacitance (μF/cm$^2$) |
|---|---|---|---|---|
| 1 | 45 | 60–60–30–30 | 120 | 330 |
| 2 | 30 | 50–40–30–25 | 120 | 455 |
| 3 | 35 | 30–30–25–20 | 120 | 535 |

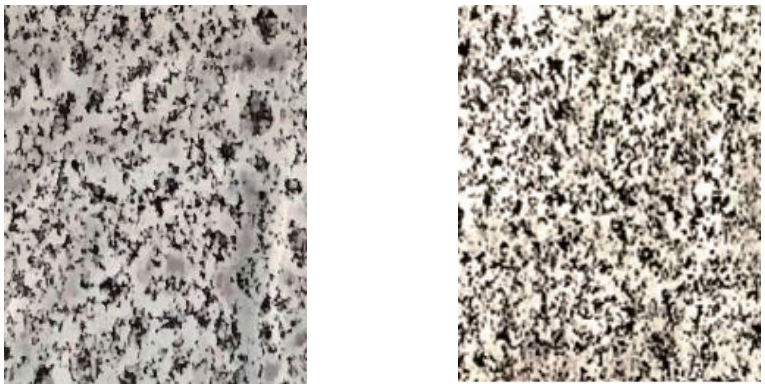

(a) (b)

Fig. 6. (Color online) Pit morphology of etched Al foil surface. Capacitances of (a) and (b) were 435 and 535 μF/cm$^2$, respectively. (a) At 35 °C for 120 s and (b) with AC under the same conditions.

When the volume of HCl in the mixed etching solution was greater than 500 mL/L, over-etching occurred, whereas a volume of less than 350 mL/L caused insufficient etching. The highest capacitance (495 μF/cm$^2$) was observed with a mixture of 350, 15, and 15 mL/L HCl, $HNO_3$, and $H_3PO_4$, respectively [Table 4, Fig. 7(a)]. Over-etching and insufficient etching lowered the capacitance of the AC-etched Al electrolytic capacitor. The addition of 5 g/L $Al^{3+}$ maximized the capacitance [Table 5, Fig. 7(b)]. When the amount of added $Al^{3+}$ was smaller than 5 g/L, rapid corrosion occurred, whereas insufficient corrosion was observed with more than 5 g/L $Al^{3+}$, which decreased the capacitance. With 5 g/L $Al^{3+}$, the capacitance increased to 512 μF/cm$^2$. With 350 mL/L HCl and 5 g/L $Al^{3+}$, the optimal current density was 0.6 A/cm$^2$, yielding a capacitance of 517 μF/cm$^2$. If it was lower than 0.6 A/cm$^2$, the etching density became lower, whereas a current density higher than 0.7 A/cm$^2$ led to excessive etching or even the dissolution of Al foil, which decreased the capacitance [Table 6, Fig. 7(c)].

At the etching solution temperature of 35 °C, etching time of 120 s, frequency of 30–30–25–20 Hz, current density of 0.6 A/cm$^2$, 5 g/L $Al^{3+}$, and 350, 15, and 15 mL/L HCl, $HNO_3$, and $H_3PO_4$, respectively, we measured the capacitance of the AC-etched Al electrolytic capacitor with the Al foil thicknesses of 104, 65, and 50 μm. When the thickness of the Al foil was 104

Table 4
Capacitance of AC-etched Al electrolytic capacitor in different mixtures of acid solutions.

| Samples | HCl (ml/L) | $HNO_3$ (ml/L) | $H_3PO_4$ (ml/L) | Capacitance (μF/cm$^2$) |
|---|---|---|---|---|
| 1 | 300 | 10 | 10 | 425 |
| 2 | 350 | 15 | 15 | 495 |
| 3 | 400 | 20 | 25 | 446 |
| 4 | 500 | 30 | 35 | 369 |
| 5 | 600 | 40 | 50 | Over-etching |

(a) (b) (c)

Fig. 7. (Color online) Pit morphology of etched Al foil surface. Capacitances of (a), (b), and (c) were 435, 512, and 517 μF/cm$^2$, respectively. (a) With mixture of 350, 15, and 15 mL/L HCl, and $HNO_3$, and $H_3PO_4$, respectively, (b) with 5 g of $Al^{3+}$, and (c) at current density of 0.6 A/cm$^2$.

Table 5
Capacitance of AC-etched Al electrolytic capacitor with different $Al^{3+}$ concentrations in etching solutions.

| Samples | $Al^{3+}$ (g/L) | Capacitance (μF/cm$^2$) |
|---|---|---|
| 1 | 1 | 468 |
| 2 | 2 | 475 |
| 3 | 3 | 484 |
| 4 | 4 | 491 |
| 5 | 5 | 512 |
| 6 | 6 | 497 |
| 7 | 7 | 381 |
| 8 | 8 | 173 |

Table 6
Capacitance of AC-etched Al electrolytic capacitor with different current densities.

| Samples | Current density (A/cm$^2$) | Capacitance (μF/cm$^2$) |
|---|---|---|
| 1 | 0.4 | 229 |
| 2 | 0.5 | 352 |
| 3 | 0.6 | 517 |
| 4 | 0.7 | 437 |
| 5 | 0.8 | 352 |
| 6 | 0.9 | 125 |

μm, its purity was 99.99%, and all the lattices showed that the arrangement direction of [422] constituted 100%. When the thicknesses were 65 and 50 μm, the purities were 99.97 and 99.91%, and the lattice orientations were [220] and [100], respectively (Table 7, Fig. 8). The average

Table 7
Capacitance of AC-etched Al electrolytic capacitor with Al foil thicknesses of 104, 65, and 50 μm.

| Samples | Capacitance (μF/cm$^2$) | | |
|---|---|---|---|
| | 104 μm | 65 μm | 50 μm |
| 1 | 499 | 496 | 511 |
| 2 | 503 | 488 | 509 |
| 3 | 486 | 506 | 506 |
| 4 | 493 | 528 | 527 |
| 5 | 489 | 495 | 498 |

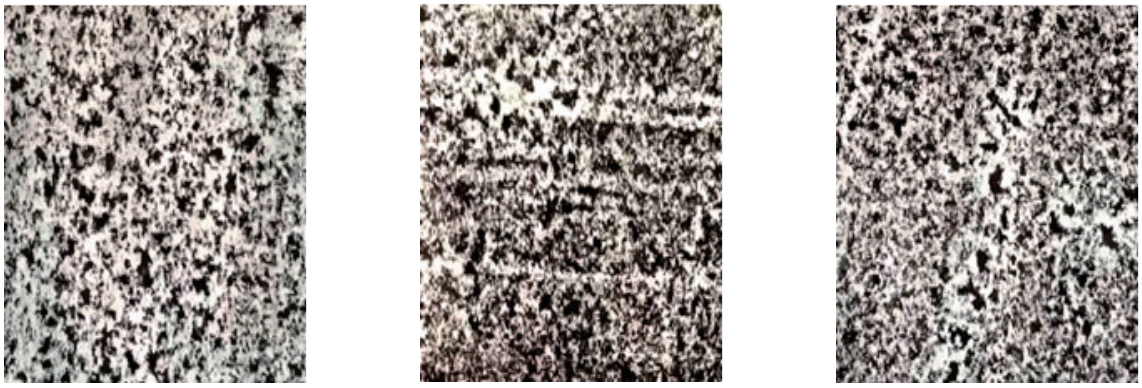

(a) (b) (c)

Fig. 8. (Color online) Pit morphology of etched Al foil surface. The average capacitances of Al foil with thicknesses of 104, 65, and 50 μm were 494, 502.6, and 510.2 μF/cm$^2$, respectively. (a) Al foil thickness of 104 μm, (b) Al foil thickness of 65 μm, and (c) Al foil thickness of 50 μm.

capacitances with different thicknesses (104, 65, and 50 μm) of Al foils were 494, 502.6, and 510.2 μF/cm$^2$, respectively. The AC-etched Al electrolytic capacitor with an Al foil of 50 μm thickness showed the highest capacitance (Fig. 8).

In summary, the highest capacitance of the AC-etched Al electrolytic capacitor was observed under the following conditions.

- Etching solution: a mixture of 350 mL/L HCl, 15 mL/L $HNO_3$, 15 mL/L $H_3PO_4$, and 5 g/L $Al^{3+}$
- Solution temperature: 35 °C
- Al foil thickness: 50 μm
- Al purity: 99.99%, containing trace amounts of iron (0.006%) and copper (0.002%)
- AC frequency: 30–30–25–20 Hz
- Etching time: 120 s
- Current density: 0.6A/cm$^2$.
- Lattice orientations: [220] (74%), [311] (18%), [200] (6%), and [422] (7%).

To examine the relationship between the multistage etching conditions and the resulting specific capacitance, a quantitative microstructural evaluation of the obtained SEM images was conducted. Image analysis results showed that the optimized four-stage frequency-stepping profile (30–30–25–20 Hz) yielded a highly uniform and dense distribution of sub-micrometer corrosion pits. The average pit diameter was constrained between 180 and 240 nm, with a peak pit nucleation density of approximately 4.2 × 10$^9$ pits/cm$^2$. This morphology contrasts with

traditional single-frequency AC processes, which often exhibit irregular pit diameters exceeding 500 nm owing to localized overcoalescence. Atomic force microscopy and laser profile characterizations showed that the average surface roughness increased significantly from 0.15 μm to an optimized value of 1.68 μm. The surface enlargement factor (the ratio of the effective electrochemical surface area to the nominal geometric area) reached 96.5.[12] This increase in effective surface area validates the measured specific capacitance according to the fundamental electrostatic relation $C = \varepsilon_0 \varepsilon_r A/d$. $H_3PO_4$ acts as a moderate passivation agent on the outer foil surface, forcing the electrochemical dissolution inward to maintain a high aspect ratio for the pits without reducing the thickness of the mechanical walls separating them.[13] The foil thicknesses are 50–100 μm in this study.

## 4. Discussion

The maximum specific capacitance achieved in this study (510.2 μF/cm$^2$) represents a significant improvement over standard electrochemical texturing methods found in the literature. Conventional DC etching under equivalent conditions generally yields deep but isolated tunnels, which typically caps specific capacitance values between 350–420 μF/cm$^2$ for low-voltage applications owing to large unetched interstitial areas.[5] Similarly, continuous single-frequency AC processes frequently result in pit merging, which destroys the delicate surface network and restricts capacitance gains.[6] The high capacity observed in the optimized method is attributed to the collaborative role of the multistage frequency shifting and the addition of $H_3PO_4$, which prevents local overdissolution and promotes highly uniform pit growth across multiple structural orientations.

To evaluate the performance of the four-stage frequency-stepping AC etching method developed in this study, the maximum specific capacitance obtained in this study was compared with previously reported values for aluminum foil etching processes under similar low-voltage or high-surface-area configurations (Table 8). Conventional single-stage AC or mixed DC/AC methods provide capacitances lower than 420 μF/cm$^2$ owing to localized over-etching or irregular pit development. The method in this study showed an improvement of over 20% compared with other multistage methods.[14] This improvement is attributed to the dynamic frequency stepping, starting from high frequencies (30 Hz) to initiate high-density, small-scale pit nucleation, to lower frequencies (25–20 Hz) that enable uniform, directional pit growth without destroying the surface framework.

The applicability of the developed etching method was also verified through reproducibility and mechanical integrity assessments. To evaluate reproducibility, five independent aluminum foil samples were etched under the optimized four-stage conditions (350 mL/L HCl, 15 mL/L $HNO_3$, and 15 mL/L $H_3PO_4$, 35 °C, 120 s). The resulting specific capacitances ranged from 504.8 to 514.3 μF/cm$^2$, with a coefficient of variation of less than 1.2%, showing high process reliability. Tensile strength test results of the etched foils showed that $H_3PO_4$ added as an inhibitor prevented the formation of excessive deep macropores or structural perforations. The remaining foil matrix maintained over 75% of the unetched foil's pristine tensile strength, meeting the standard handling and winding mechanical requirements for industrial capacitor manufacturing.

Table 8
Comparison of specific capacitances and etching parameters with representative values in the literature.

| Etching method | Solution | Maximum specific capacitance ($\mu F/cm^2$) |
|---|---|---|
| Single-stage AC (50 Hz)[15] | $HCl + HNO_3$ | 320.5 |
| Multistep DC + AC etching[14] | $HCl + H_2SO_4$ | 415 |
| Constant high-frequency AC (60 Hz)[16] | $HCl + H_3PO_4$ | 385.2 |
| Four-stage frequency-stepping (30–30–25–20 Hz) | $HCl + HNO_3 + H_3PO_4$ | 510.2 |

To validate the performance of the fabricated aluminum electrolytic capacitors, electrical and reliability characteristics, equivalent series resistance (ESR), frequency response, and leakage current reliability were evaluated. The ESR of the capacitor fabricated using the optimized four-stage frequency-stepping etched foil was measured across a standard operating range. At a frequency of 120 Hz, the device exhibited an exceptionally low ESR of 0.12 Ω, which is approximately 25–30% lower than those of capacitors fabricated via traditional single-stage AC etching methods.[17] This reduction in ESR is attributed to the uniform, interconnected network of corrosion pits generated by introducing the 30–30–25–20 Hz step-down frequency profile and $H_3PO_4$. This optimized morphology minimizes the constriction resistance of the electrolyte within the microtunnels and ensures continuous contact pathways.

The frequency response of the specific capacitance was evaluated from 100 Hz to 10 kHz. As expected for porous electrochemical structures, a capacitance roll-off was observed at high frequencies owing to the limited penetration depth of ions into the deep sub-micrometer tunnels. However, the optimized foil retained over 68% of its nominal 120 Hz capacitance at 1 kHz, showing superior frequency stability over deep tunnel-type DC-etched foils, whose capacitance typically drops below 50% owing to highly restricted, long diffusion paths.[18]

Long-term reliability was assessed using leakage current stability and accelerated life testing (85 °C at a rated voltage of 6.3 V for 1000 h). The initial leakage current was stabilized at a low baseline of 0.012 μA/μF·V. After the 1000-h continuous stress test, the capacitance degradation was confined to less than 4.5%, and no dielectric breakdown or significant ESR spike was observed. This confirms that the uniform oxide layer grown on the well-distributed, non-overlapping pit structures possesses excellent chemical and structural stability, satisfying the rigorous demands of industrial sensing and power-filtering circuits.

## 4. Conclusions

Appropriate texturing of aluminum foils is fundamental to achieving high volumetric efficiency and operational reliability in electrolytic capacitors, particularly for advanced sensor technologies. In this study, we established optimal etching parameters: foil thickness of 50 μm, a multi-acid solution (350 mL/L HCl, 15 mL/L $HNO_3$, 15 mL/L $H_3PO_4$, and 5 g/L $Al^{3+}$) at 35 °C, a four-stage AC frequency profile (30–30–25–20 Hz), an etching time of 120 s, and a current density of 0.6 A/cm², which collectively enabled superior performance outcomes. The optimized etching process enhanced the effective electrochemical surface area by a factor of 96.5, producing a uniform, ultradense pit array (180–240 nm diameter, $4.2 \times 10^9$ pits/cm$^2$) without

structural collapse. This morphology yielded a specific capacitance of 510.2 μF/cm² with excellent reproducibility (coefficient of variation < 1.2%), maintaining over 75% of the foil's original tensile strength due to the buffering action of $H_3PO_4$. Electrical characterization confirmed the exceptionally low ESR (0.12 Ω at 120 Hz) and strong high-frequency retention (68% capacitance at 1 kHz). Long-term reliability testing under thermal stress (85 °C, 6.3 V, 1000 h) demonstrated remarkable durability, limiting capacitance degradation to under 4.5%.

These results underscore the role of precise microstructural control in balancing capacitance, mechanical integrity, and reliability. The robustness of the AC-etched Al electrolytic capacitor directly addresses challenges posed by weathering, chemical exposure, and aging, ensuring resilience in harsh environments. The results of this study support the trend toward miniaturization and integrated hardware, delivering dependable, long-life energy buffering components essential for next-generation intelligent sensing, automotive modules, and pervasive low-power wireless sensor networks.

## References


1 TDK: https://www.tdk-electronics.tdk.com/download/185386/af1debd2b2e96735fb128efc485dd086/pdf-generaltechnicalinformation.pdf (accessed August 2025).
2 Nichicon: https://www.nichicon.com/en-us/news-and-resources/news-technical-articles/trends-involving-cutting-edge-automotive-aluminum-electrolytic-capacitor-technology/ (accessed August 2025).
3 P. Wang, D. Li, X. Shen, Y. Liu, D. He, R. Liu, Y. Xie, and L. Xiong: J. Energy Storage **169** (2026) 122797. https://doi.org/10.1016/j.est.2026.122797
4 T. Zhu, G. Feng, L. Ning, and N. Peng: J. Mater. Sci. **60** (2025) 7117. https://doi.org/10.1007/s10853-025-10879-6
5 T. Xie, X. Liu, W. Yang, Y. Ji, J. Wu, and C. Dong: Int. J. Electrochem. Sci. **21** (2026) 101447. https://doi.org/10.1016/j.ijoes.2026.101447
6 N. Osawa: Corros. Mater. Degrad. **6** (2025) 10. https://doi.org/10.3390/cmd6010010
7 R.-G. Xiao, K-P. Yan, J.-X. Yan, and J.-Z. Wang: Corros. Sci. **50** (2008) 1576. https://doi.org/10.1016/j.corsci.2008.02.017
8 B. Hu, Y. Sun, B. Guan, J. Zhao, H. Zhang, D. Zhu, and C. Cheng: App. Surf. Sci. **392** (2017) 375. https://doi.org/10.1016/j.apsusc.2016.09.074
9 Y. L. Lee, B. L. Ou, and H. C. Yi: J. Mater. Sci. Mater. Electron. **18** (2007) 627. https://doi.org/10.1007/s10854-006-9058-7
10 K. Nishio, T. Yanagishita, M. Yoshida, T. Hayakawa, and H. Masuda.: Electrochem. Commun. **59** (2015) 13. https://doi.org/10.1016/j.elecom.2015.06.017
11 C.-L. Ban, J.-H. Chen, F.-R. Wang, S.-Q. Zhu, and Z.-Q. Liu: J. Nanosci. Nanotechnol. **19** (2019) 7471. https://doi.org/10.1166/jnn.2019.16721
12 J. Scherer, O.M. Magnussen, T. Ebel, and R.J. Behm: Corros. Sci. **41** (1999) 35. https://doi.org/10.1016/S0010-938X(98)00128-0
13 R. Zhao, R. Hauert, R. Crockett, C. Cancellieri, S. Gaan, P. Schmutz, M. Heuberger, and L. P. H. Jeurgens: Appl. Surf. Sci. **667** (2024) 160363. https://doi.org/10.1016/j.apsusc.2024.160363
14 J. Wu, Y. Xi, W. Yang, P. Liu, K. Dong, B. Zhang, C. Dong, and J. Wu: J. Mater. Res. Technol. **42** (2026) 2258. https://doi.org/10.1016/j.jmrt.2026.03.207
15 H.-J. Oh, J.-H. Lee, H.-J. Ahn, Y. Jeong, N.-J. Park, S.-S. Kim, and C.-S. Chi: Mater. Sci. Eng. A **449–451** (2007) 348. https://doi.org/10.1016/j.msea.2006.01.159
16 M. R. Arora, E. J. Paquette, and A. B. McPherson: US Patent No. US4330652A (1981). https://patents.google.com/patent/US4332652A/en
17 F. G. Hayatee: Act. Passiv. Electron. Compon. **2** (1974) 67. https://doi.org/10.1155/APEC.2.67
18 T. Yanagishita, M. Imaizumi, T. Kondo, and H. Masuda: Electrochem. Commun. **78** (2017) 26. https://doi.org/10.1016/j.elecom.2017.03.019